Journal of Structural Biology 183 (2013) 312–319

Contents lists available at ScienceDirect

Journal of Structural Biology

journal homepage: www.elsevier.com/locate/yjsbi

The guanine nucleotide exchange factor Rlf interacts with SH3 domain-containing proteins via a binding site with a preselected conformation

Milica Popovic [a], Arjen J. Jakobi [b], Marije Rensen-de Leeuw [a], Holger Rehmann [a,*]

[a] Department of Molecular Cancer Research, Centre of Biomedical Genetics and Cancer Genomics Centre, University Medical Center Utrecht, Utrecht, The Netherlands
[b] Department of Crystal and Structural Chemistry, Bijvoet Center for Biomolecular Research, Utrecht University, The Netherlands

ARTICLE INFO

Article history:
Received 14 May 2013
Received in revised form 5 July 2013
Accepted 15 July 2013
Available online 24 July 2013

Keywords:
Rlf/Rgl2
Crystal structure
SH3 domain
Pre-selected binding conformation
Small G-protein
Guanine nucleotide exchange factor

ABSTRACT

Rlf is a guanine nucleotide exchange factor for the small G-proteins RalA and RalB and couples Ras- to Ral-signalling. Here the crystal structure of the catalytic module of Rlf consisting of a REM- and a CDC25-homology domain is determined. The structure is distinguished by an extended three stranded β-sheet called the flagpole. The flagpole is a conserved element in the RalGDS family of guanine nucleotide exchange factors and stabilises the orientation of the REM-domain relative to the CDC25-homology domain. A proline-rich sequence in the flagpole is unique to Rlf and several proteins that interact with this sequence by SH3 domains are identified. Conformational pre-selection results in a gain of affinity and contributes to the establishment of SH3 domain selectivity.

1. Introduction

The members of the Ras-family of small G-proteins are involved in the regulation of such diverse effects as proliferation, differentiation, adhesion and exocytosis. They do so by acting as molecular switches cycling between an off- and an on-state, whereby the latter mediates downstream signalling. The off-state corresponds to the GDP-bound version and the on-state to the GTP-bound version of the G-protein. Transition to the on-state is caused by the exchange of GDP for GTP. Nucleotide exchange is catalysed by guanine nucleotide exchange factors (GEFs). Switching off is achieved by the hydrolysis of GTP to GDP. The intrinsically low GTPase activity of small G-proteins is enhanced by GTPase activating proteins (GAPs), which terminate signalling. Effector proteins selectively interact with the GTP bound conformation of the G-protein and are responsible for transmitting the signal (Vetter and Wittinghofer, 2001; Bos et al., 2007; Wennerberg et al., 2005).

The small G-protein Ral is involved in the control of exocytosis (Moskalenko et al., 2002), endocytosis (Jullien-Flores et al., 2000), gene regulation (de Ruiter et al., 2000) and cellular transformation (Urano et al., 1996;White et al., 1996). The RalGDS family of GEFs connects signalling of the small G-proteins Ras and Ral and consists of four members in human: Rgl1, Rlf/Rgl2, Rgl3, and RalGDS. In all family members an N-terminal REM-domain is followed by a CDC25 homology domain (CDC25-HD) and a C-terminal RA-domain. CDC25-HDs are the catalytic domains found in GEFs for members of the Ras-family of small G-proteins (Quilliam et al., 2002). The CDC25-HDs of the RalGDS family are selective for the small G-proteins RalA and RalB (Albright et al., 1993; Wolthuis et al., 1997; Ferro et al., 2008). REM-domains co-occur with CDC25-HDs. REM-domains mainly stabilise the fold of the CDC25-HD (Quilliam et al., 2002) but the REM-domain of SOS, a GEF for Ras, is also involved in allosteric regulation (Sondermann et al., 2004). RA-domains bind to the GTP-bound form of Ras- and Rap-proteins (Herrmann, 2003). Thereby GEFs of the RalGDS family act mainly as effectors of Ras-signalling, as they are recruited by Ras•GTP to membrane compartments where Ral is localised as well.

SH3 domains interact with proline-rich sequences with the minimal consensus being PxxP (Kay et al., 2000). About 300 SH3 domains are found in the human genome. This number highlights the evolutionary success in using small domains as modules, which can be shuffled and integrated into many genes, as a tool to create protein interactions. This process is further eased by the need of only a short stretch of about seven residues containing a PxxP motif as the requirement for SH3 domain binding in the target

* Corresponding author. Address: Department of Molecular Cancer Research, Centre of Biomedical Genetics and Cancer Genomics Centre, University Medical Center Utrecht, Universiteitsweg 100, 3584 CG Utrecht, The Netherlands.
E-mail address: h.rehmann@umcutrecht.nl (H. Rehmann).

1047-8477/$ - see front matter © 2013 Elsevier Inc. All rights reserved.
http://dx.doi.org/10.1016/j.jsb.2013.07.009

protein. On the other hand this raises the question whether elements other than the primary structure surrounding the proline residues contribute to the establishment of selectivity.

Here the crystal structure of the catalytic module of Rlf is determined. An exposed SH3 domain binding site is predicted from the structure and indeed, several SH3 domain-containing proteins are identified in a yeast two-hybrid screen and confirmed to interact with the exposed binding site in Rlf.

2. Material and methods

2.1. Constructs

The SH3 domains of PLCγ-1 (PLCG1, *homo sapiens*, aa 790–848) referred to as PLCγ-1^{SH3}, myosin-1E (MYO1E, *homo sapiens*, aa 1054–1108) and intersectin-2 (ITSN2, *homo sapiens*, aa 1117–1185) were cloned into the pGEX4T3 expression vector. Amino acid residues 1–778, 1–735, 50–735 or 50–514 of Rlf (Rgl2, *mus musculus*) were cloned into the pGEX6P3 expression vector. cDNAs for PLCγ-1 (IRAKp961M0798Q) and myosin-1E (IRATp970C10100D) were obtained from Source BioScience and cDNAs for intersectin-2 (Addgene plasmid 25174) from Addgene.

2.2. Protein purification

Ral and the SH3 domains of PLCγ-1, myosin-1E and intersectin-2 were expressed and purified as GST fusion proteins according to standard procedures, if required, the GST-tag was removed by thrombin cleavage. H-Ras (*homo sapiens*, aa 1–166) was expressed from the ptac plasmid and loaded with the hydrolysis resistant GTP analogue GppNHp as described (Herrmann et al., 1996).

Rlf proteins were expressed as GST fusion proteins in the bacterial strain CK600K upon induction with 100 μM IPTG at 25 °C over night in Standard I medium (Merck). The bacteria were harvested by centrifugation, re-suspended in buffer containing 50 mM Tris HCl pH 7.5, 50 mM NaCl, 5 mM EDTA, 5% glycerol, 5 mM β-mercaptoethanol and 0.1 mM PMSF and lysed by sonication. The lysate was cleared by centrifugation at 50,000*g* and loaded to a GSH column (Pharmacia) equilibrated with the previous buffer. The column was washed with 6 column volumes of buffer containing 50 mM Tris HCl pH 7.5 400 mM NaCl, 5% glycerol and 5 mM β-mercaptoethanol, with 20 column volumes of buffer containing 50 mM Tris HCl pH 7.5, 100 mM KCl, 10 mM $MgCl_2$, 5% glycerol, 5 mM β-mercaptoethanol and 0.25 mM ATP at low flow rate, with two column volumes of 50 mM Tris HCl pH 7.5, 50 mM NaCl 2,5% glycerol and 5 mM β-mercaptoethanol (buffer A) and eluted with buffer A containing 20 mM glutathione. The protein containing fractions were pooled, concentrated, supplemented with 1 mg homemade GST-PreScission Protease per 100 mg protein, dialysed against buffer A and re-applied to a GST column equilibrated with buffer A, concentrated and further purified by gel filtration on a Superdex75 26/60 column (GE-Healthcare) in buffer A.

2.3. Crystallography

Rlf^{fl}, Rlf$^{1-735}$, Rlf$^{50-735}$ and Rlf$^{50-514}$ were subjected to crystallisation trials. Only Rlf$^{50-514}$ resulted in crystals. The initial hit was optimised and final crystals were grown at 289 K in sitting drops using a reservoir solution containing 0.1 M Bis–Tris propane, pH 6.5, 0.2 M $NaNO_3$ and 12% PEG 3350. Crystals were cryoprotected in a solution containing the mother liquor supplemented with 20% glycerol and flash cooled in liquid nitrogen. Data were collected at 100 K at beamline ID23eh1 of ESRF and processed with XDS (Kabsch, 1993). Molecular replacement was carried out in MOLREP (Vagin and Teplyakov, 2000) using the CDC25-HD of RalGPS1 (residues 23–289) and RasGRF1 (1028–1262) (residues 482–991) as poly-alanine search model. The program O (Jones et al., 1991) was used to build the model into 2Fo-Fc and Fo-Fc maps and refinement was carried out with REFMAC (Murshudov et al., 1997). Residues 195–203, 215–230, 273–282, 389–396, 403–426 and 513–514 of molecule A and 50–52, 75–81, 195–203, 218–233, 389–398 and 403–426 of molecule B are not visible. The Ramachandran plot depicts 94.7% of main chain torsion angles in the most favoured and 5.3% in additional allowed regions with 0 residues in disallowed regions.

Figures were generated using the programs Molscript (Kraulis, 1991), Bragi (Schomburg and Reichelt, 1988) and Raster3D (Merritt and Murphy, 1994).

2.4. Determination of GEF activity

RalB was loaded with the fluorescent GDP analogue 2′-/3′-O-(N-methylanthraniloyl)-guanosine diphosphate (mGDP) as described previously for Rap1B (Rehmann, 2006). The fluorescence intensity of Ral bound mGDP is approximately twice as intense as of free mGDP and thus nucleotide exchange can be observed as decay in fluorescence upon addition of an excess unlabelled GDP. All reactions were performed in buffer containing 50 mM TrisHCl pH7.5, 50 mM NaCl, 5 mM $MgCl_2$, 5 mM DTT, 5% glycerol and 20 μM GDP at 20 °C, with 200 nM Ral•mGDP and 50 nM Rlf as described (Rehmann, 2006). Ras•GppNHp and PLCγ-1^{SH3} were added at concentration as indicated in the figure legends.

2.5. Yeast two-hybrid

A human placenta cDNA library was screened for Rlf interacting proteins by Hybrigenics, SA, Paris, France.

2.6. Isothermal titration calorimetry

Titrations were performed in a NANO ITC 2G (TA Instruments) equipped with a 1 ml cell at 20 °C. In a typical experiment a solution of 190 μM Rlf$^{50-514}$ or GST-Rlf$^{79-91}$ was titrated with a solution of 1.5 mM PLCγ-1^{SH3} in steps of 6 μl. Experiments were performed in buffer containing 50 mM TrisHCl pH 7.5, 50 mM NaCl, 2.5% glycerol and 0.5 mM Tris(2-carboxyethyl)phosphine hydrochloride. All proteins were brought into buffer of the same preparation either by gel filtration or by extensive dialysis. Data were analysed by the manufacturer's software.

2.7. Co-precipitation assays

GST or GST-fusion proteins from lysates of bacteria overexpressing the respective proteins were coupled to glutathione beads and washed three times with buffer containing 50 mM Tris-HCl pH 7.5, 50 mM NaCl, 2% glycerol and 5 mM β-mercaptoethanol. 20 μg of Rlf$^{50-514}$ or Rlf$^{50-514}$R87E, or buffer control, were added to the pre-coupled beads and incubated for 20 min at room temperature under gentle tumbling. The beads were washed three times with buffer as before and eluted by application of 18 μl of Laemmli loading buffer and heating to 95 °C for three minutes. The samples were subjected to analysis by SDS–PAGE on 12.5% gels and protein bands were stained by Coomassie Brilliant Blue.

2.8. Coordinates

Coordinates and structure factors have been deposited in the Protein Data Bank with the accession code 4JGW.

3. Results

3.1. Crystal structure of Rlf$^{50-514}$

Several constructs of Rlf were subjected to crystallisation trials of which Rlf$^{50-514}$ resulted in crystals suitable for structure determination (Table 1). Rlf$^{50-514}$ contains the REM-domain and the CDC25-HD but lacks the far N-terminus, which is expected to be unstructured, and the C-terminal RA-domain. In agreement with earlier studies on Rgl1 (Murai et al., 1997) Rlf$^{50-514}$ is fully functional in terms of its catalytic activity towards Ral (Fig. 1). Furthermore, addition of Ras or Rap loaded with a non-hydrolysable GTP analogue has no effect on the activity of full length Rlf (Fig. 1 and not shown). This confirms the classification of Rlf as a constitutively active GEF, whereby the interaction of Ras•GTP with the RA domain results in translocation of Rlf rather than in an allosteric regulation of the GEF activity itself.

Rlf$^{50-514}$ crystallised in space group $P2_1$ with two molecules per asymmetric unit. Differences between the two molecules are mainly restricted to the N-terminal β-sheet (Suppl. Fig. 1A). The two molecules are related approximately by a twofold non-crystallographic axis through a contact interface in the CDC25-HD (Fig. 2). In gelfiltration the majority of Rlf$^{50-514}$ appears as monomer, whereas a minority is found in a dimeric or oligomeric state. Single mutations in the contact interface, which abolish crystal formation, do not influence the behaviour in gelfiltration. It is therefore unlikely that the crystallographic dimer interface is of physiological relevance.

Table 1
Crystallographic data.

Data collection		Refinement	
Space group	$P2_1$	Resolution range (Å)	31–2.3
Cell dimensions (Å)	a = 70.9 b = 75.6 c = 101.3	R_{cryst} (%)	25.2
Cell angels (°)	α = 90 β = 98.1 γ = 90	R_{free}[b] (%)	28.8
Wavelength (Å)	0.97626	Average B factor (Å^2)	42.2
Resolution range (Å)[a]	31–2.3 (2.4–2.3)	Rmsd from ideal values:	
Number of reflections	220886	Bond lengths (Å)	0.007
Number unique reflections	46676	Bond angles (°)	0.998
Completeness (%)a	98.6 (98.2)		
I/α[a]	24.3 (3.4)		
R_{meas}[a] (%)	4.6 (47.0)		

[a] Values in parenthesis correspond to highest resolution shell.
[b] The Free-R factor was calculated with 5% of the data omitted from structure refinement.

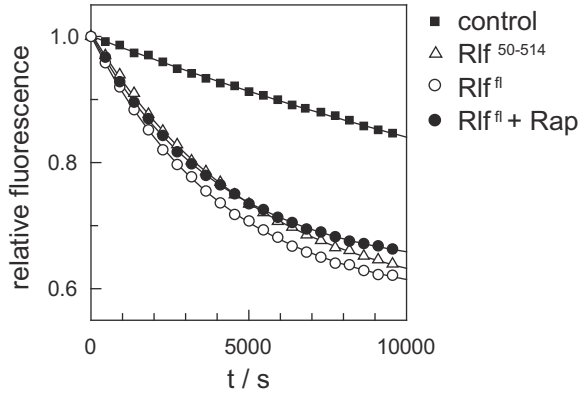

Fig.1. The activity of Rlf is independent of its RA domain. Nucleotide exchange activity of 50 nM full length Rlf (Rlf^{fl}) in the presence or absence of 10 μM Rap•GppNHp, or Rlf$^{50-514}$ towards RalB was measured as decay in the fluorescence signal caused by the exchange of a fluorescent GDP analogue bound to Ral.

The CDC25-HD of Rlf distinguishes itself from previously crystallised CDC25-HDs (Boriack-Sjodin et al., 1998; Rehmann et al., 2006; Freedman et al., 2006) by two insertions spanning residues 307–322 and 402–427. Both insertions are at solvent exposed regions. Residues 403–426 are unstructured. Residues 307–322 form a β-strand-loop-β-strand structure, which is inserted between two α-helices (Fig. 2B). The insertions are distant to the catalytic site. The catalytic site of the CDC25-HD can be assigned based on the structures of SOS1•H-Ras (Boriack-Sjodin et al., 1998) and Epac2•Rap1B (Rehmann et al., 2008). The catalytic site is freely accessible for binding to Ral (Fig. 2B and S1B). In analogy to the structures of SOS1 and Epac2, the α-helix formed by residues 432–444 would be inserted into the nucleotide binding cleft of Ral (Suppl. Fig. 1B). This α-helix is the N-terminal α-helix of the so-called helical hairpin, a helix-loop-helix structure. As the helical hairpin protrudes out of the CDC25-HD, the loop between the two helices is referred to as "the tip-loop".

An important function of the REM-domain is the stabilisation of the helical hairpin. The REM-domain shields the hydrophobic residues Phe457 and I455 in the C-terminal helix of the helical hairpin (Fig. 3). Both residues are conserved in CDC25-HDs. In variance to SOS1 and Epac2, the interaction is additionally stabilised by Phe464 and Tyr454, which function like cantles at both ends of a saddle (Fig. 3). These residues are only conserved in the RalGDS family.

3.2. An N-terminal β-sheet protrudes out of the structure

The first forty residues of Rlf$^{50-514}$ form a striking three stranded β-sheet of some 10 residues per strand, which protrudes out of a compact unit formed by the REM-domain and the CDC25-HD (Figs. 2 and 4). Therefore the β-sheet will be referred to as "the flagpole". The flagpole is C-terminally directly connected to the first helix of the REM-domain (Fig. 4A). The last residues of the third β-strand anchor the REM-domain to the CDC25-HD and stabilise the relative orientation between these domains. They are therefore referred to as "the anchor". The anchor forms a β-sheet-like interaction with the tip-loop of the helical hairpin in the CDC25-HD. The tip-loop expands the flagpole β-sheet by two short "pseudo"-β-strands (Fig. 4A).

The same anchoring mechanism is found in SOS1 and Epac2 (Fig. 4B and C). The tip-loop of the helical hairpin in SOS1 is longer by some residues than in Epac2 or Rlf and forms two clear, albeit short β-strands. The anchor in SOS1 is a short β-strand on its own and not the end of a long β-strand as in Rlf (Fig. 4C). In SOS1 the β-sheet formed by the tip-loop and the anchor is extended by a β-sheet-like interaction with a short sequence element N-terminal to the anchor. Structurally this element mimics the N-terminus of the second β-strand of the flagpole (Fig. 4C). Epac2 contains a structural element that could be considered as a short version of the flagpole. As in Rlf a three stranded β-sheet is extended by a β-sheet-like interaction with the tip-loop of the helical hairpin (Fig. 4B).

3.3. Rlf contains a binding site for SH3 domains

The loop between the second and the third β-strand of the flagpole in Rlf contains a proline-rich sequence (Figs. 2, 4A). At the top of the flagpole, the loop is highly exposed and accessible and could thus function as a binding site for SH3 domains. Indeed, a yeast two-hybrid screen with Rlf had identified the SH3 domain-contain-

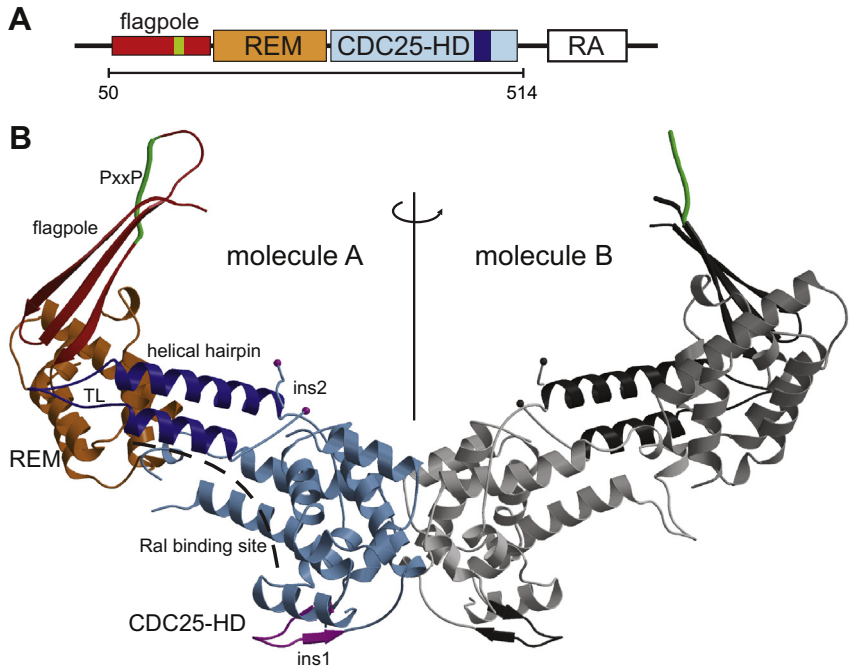

Fig.2. Crystal structure of Rlf$^{50-514}$. (A) Domain organisation of Rlf. The colour code is used throughout the figures. REM, Ras Exchange Motif; CDC25-HD, CDC25-homology domain; RA, Ras-Association. (B) Ribbon diagram of the crystallographic dimer of Rlf$^{50-514}$, with molecule A coloured as coded in (a) and molecule B in shades of gray. The twofold rotation axis is indicated. The predicted binding site for Ral in the CDC25-HD is indicated by dotted line. Rlf specific insertions in the CDC25-HD are highlighted in magenta and are labelled ins1 (aa 307–322) and ins2 (aa 403–426, start and end position indicated; the residues itself are unstructured). PxxP, proline-rich region (aa 82–87) are represented by thick coil in green; TL tip loop within the helical hairpin.

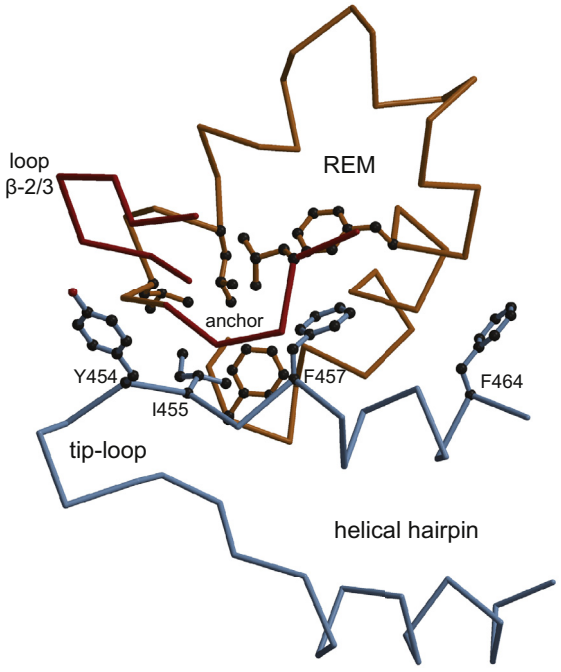

Fig.3. Hydrophobic interaction between the REM-domain and the CDC25-HD. Parts of the REM-domain (orange) which are shielding Ile455 and Phe457 are shown. Phe464 and Tyr454 are stabilising the position of the REM-domain. Loop β2/β3 refers to the loop between β-strand 2 and 3 of the flagpole. (For interpretation of the references to colour in this figure legend, the reader is referred to the web version of this article.)

ing proteins PLCγ-1, myosin-1E and intersectin-2 as Rlf interacting proteins. Whereas PLCγ-1 and myosin-1E contain one SH3 domain each, intersectin-2 contains five SH3 domains. Sequence analysis indicates highest homology between the SH3 domains of PLCγ-1, myosin-1E and the fifth SH3 domain of intersectin-2 (Suppl. Fig. 2A). These SH3 domains display the sequence features for binding to PxPPxR motives (Suppl. Fig. 2A). Such a motive is found in the flagpole P_{76}LDPLA**PLPPP**$\mathbf{R}_{87}$. The interaction between Rlf and the hits of the yeast two-hybrid screen were confirmed by the ability of the isolated SH3 domains to co-precipitate Rlf$^{50-514}$ (Fig. 5A).

Next to the proline-rich sequence in the flagpole, the region from residue 217–236 in the unresolved linker region between the REM-domain and the CDC25-HD contains several proline residues and several additional PxxP motives are found distributed over the protein. Isothermal titration calorimetry (ITC) in combination with a mutagenesis study was used to assign the SH3 domain binding site in Rlf unambiguously. The SH3 domain of PLCγ-1 (PLCγ-1^{SH3}) was selected for more detailed analysis. PLCγ-1^{SH3} binds to Rlf$^{50-514}$ and to Rlf$^{75-91}$ with 0.9 μM and 16 μM affinity, respectively, indicating that the proline-rich sequence of the flagpole is sufficient for binding (Fig. 5B). No heat-traces were observed upon titration of PLCγ-1^{SH3} into solutions of Rlf$^{50-514}$ containing the mutations P82E, P84E or R87E (Fig. 5C). In precipitation experiment neither PLCγ-1^{SH3} nor the SH3 domain of myosin1E or the fifth SH3 domain of intersectin2 is able to interact with Rlf$^{50-514}$R87E, indicating that the flagpole is the docking site for all three proteins.

3.4. The SH3 domain-binding site is in a preselected conformation

The peptide (RPK**P**V**PPPR**G) bound to the SH3 domain of myosin I from *Acanthamoeba castellanii* (pdb entry 2DRK) can be superimposed onto the mapped binding site in Rlf ($\mathbf{P}_{82}$L**PPPR**$_{87}$) (Fig. 6A and B). Pro82, Pro84 and Arg87 in Rlf would point into the hydrophobic cleft of the SH3 domain and glutamic acid at these positions would be incompatible with binding, which is in agreement with the mapping studies. The PLPPPR motif in Rlf adopts a

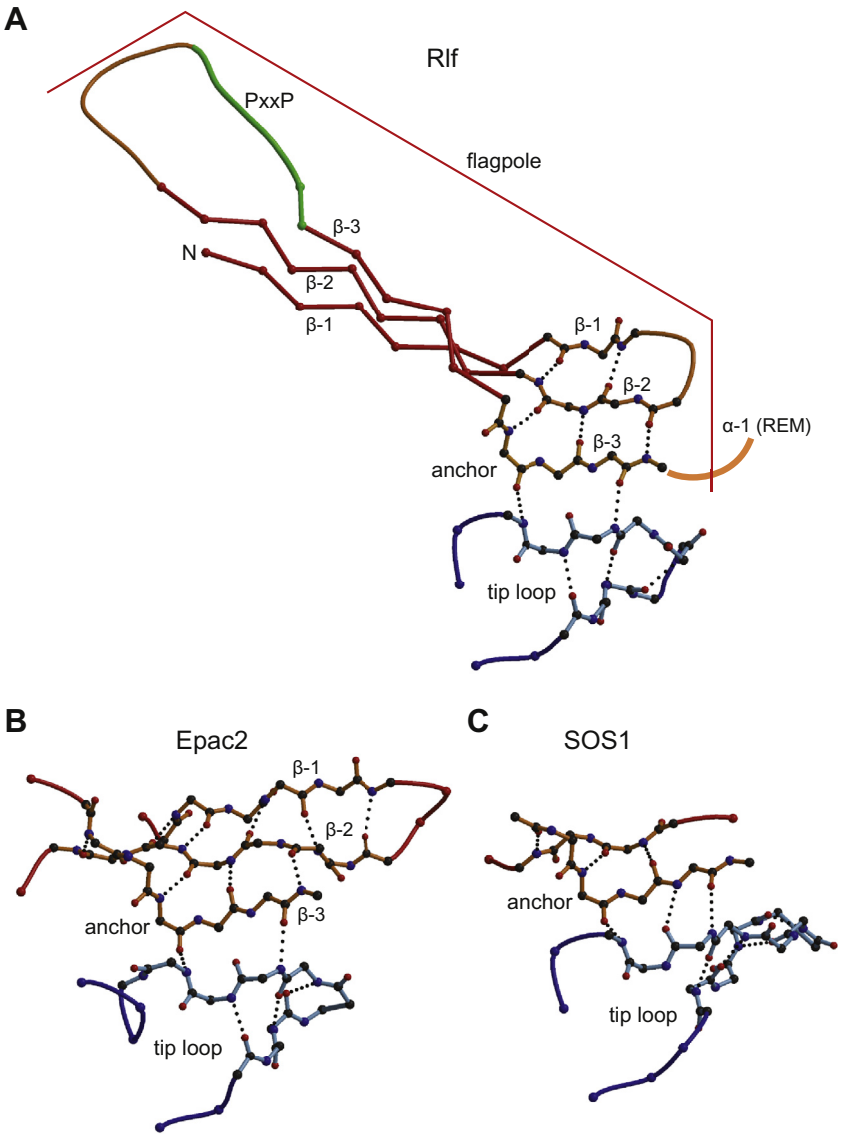

Fig.4. The flagpole and its relation to the CDC25-HD. (A) The three stranded β-sheet formed by residues 53–95 is shown with the individual strands labelled β1, β2 and β3. The last residues of β3, labelled as anchor, form a β-sheet-like interaction with the tip-loop (blue) of the helical hairpin and are connected to the first α-helix of the REM-domain as graphically indicated. Residues, which are involved in this interaction, are shown in ball-and-stick representations with the side chains omitted for clarity. Dotted lines indicate hydrogen bonds. PxxP, proline-rich region (residues 82–87) are represented by thick coil in green. N, N-terminus. (B, C) The structural equivalent elements in Epac2 (B) and SOS1 (c) are show. Note, the equivalent to β1 is missing in SOS1. All three panels are at the same scale and in the same orientation based on superposition of the CDC25-HDs. (For interpretation of the references to colour in this figure legend, the reader is referred to the web version of this article.)

conformation ready to accept binding of an SH3 domain (Fig. 6B). Furthermore, the engagement of the PLPPPR motif in the end of the first β-strand and the following loop is basically compatible with an SH3 domain interaction. Binding in this docking pose would only require a slight adaptation in the loop region following the PLPPPR motif as judged from the loop conformation in molecule A of the asymmetric unit (Fig. 6A). In molecule B this loop region is unresolved. The remaining parts of the flagpoles including the proline motif are highly similar in both molecules, except a slight difference in the angle by which the flagpoles protrude (Fig. 6C and S1A). This is indicative for an intrinsic conformational flexibility within the loop region, which would likely allow adaption for SH3 domain binding in the proposed docking pose.

The docking pose suggests the absence of additional contacts between Rlf and a bound SH3 domain except the interaction with the PLPPPR motif as the flagpole keeps the SH3 domain distant to the remaining molecule (Fig. 6A). In agreement with this is the catalytic activity of Rlf^{50-514} not influenced by binding of $PLC\gamma-1^{SH3}$ (Fig. 5D).

4. Discussion

The flagpole is a distinctive element in the structure of Rlf. Sequence analysis suggests that the flagpole is a common element in the RalGDS family (Suppl. Fig. 2B). Even though sequence homology is only moderate in this region, secondary structure prediction supports the existence of the β-sheet. The proline-rich sequence in the loop between the second and the third β-strand is, however, unique in Rlf/Rgl2 (Suppl. Fig. 2B).

The flagpole can be considered as an independent structural element N-terminal to the REM-domain. In agreement with this, sequence based automated domain assignments as the SMART-algorithms define the N-terminus of the first helix in the REM-domain as the start of the domain. However, the anchor is crucial in

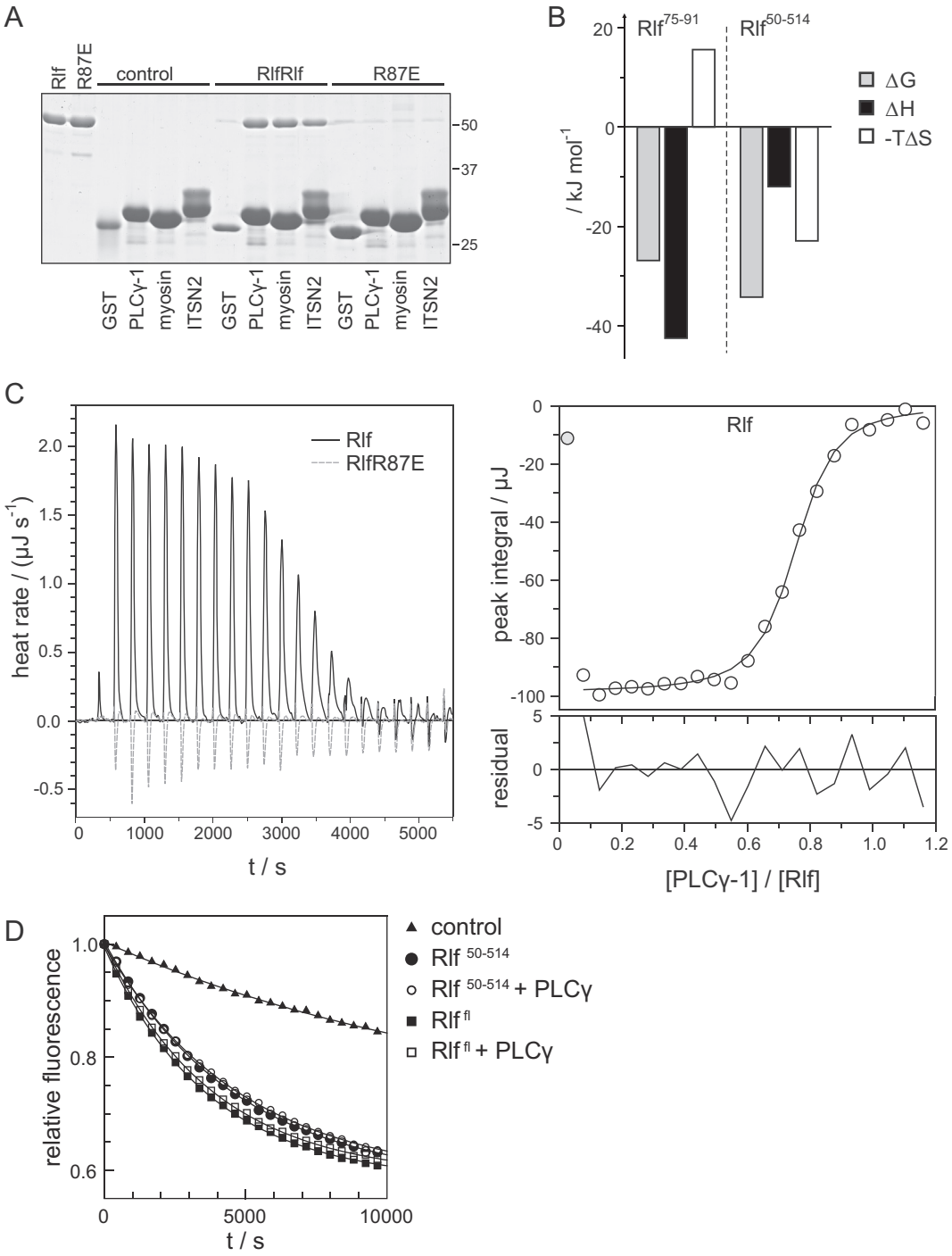

Fig.5. Interaction between Rlf and SH3 domains. (A) GST-fusion proteins of the SH3 domains of PLCγ-1, myosin1E and intersectin2 (ITSN2) were immobilised on glutathione beads and used to precipitate either Rlf^{50-514} (Rlf) or Rlf^{50-514}R87E (Rlf R87E). Rlf^{50-514} and Rlf^{50-514}R87E were loaded to the first two lanes as reference. Shown is a Coomassie Briliant Blue-stained SDS–PAGE. (B) GST-Rlf^{75-91} or Rlf^{50-514} were titrated with PLCγ-1^{SH3} in an isothermal titration calorimeter to determine the affinity and the enthalpy of the interaction. From this the free enthalpy and the binding entropy were calculated. (C) Heat trace from the titration of 187 μM Rlf^{50-514} or Rlf^{50-514}R87E with 1.5 mM PLCγ-1^{SH3} (left) and the corresponding analysis of the interaction between Rlf^{50-514} and PLCγ-1^{SH3} (right). The peaks were integrated to obtain the heat release per injection, which is plotted against the molar ratio of the total protein concentrations. Data were fitted to a model assuming n independent binding sites and $n = 0.73$ was obtained. (D) Nucleotide exchange activity of 50 nM full length Rlf (Rlf^{fl}) or Rlf^{50-514} towards RalB in the presence or absence of 10 μM PLCγ-1^{SH3}.

stabilising the relative orientation between the REM-domain and the CDC25-HD. REM-domains co-occur with CDC25-HD (Quilliam et al., 2002) and the anchor is found in all known structures of this module (Rehmann et al., 2006; Boriack-Sjodin et al., 1998). For that reason, we had previously proposed to consider the anchor-containing β-strand as a part of the REM-domain (Rehmann et al., 2006).

This proposal is further justified by the functionality of the Rap-GEF Epac2. In Epac2 the REM-domain is preceded by a cyclic nucleotide binding domain. cAMP interacts with the core of the cyclic nucleotide binding domain as well as with the first and second β-strand of the flagpole-like structure in Epac2. Consequently these two β-strands were considered as being part of the cyclic nucleotide binding domain (Rehmann et al., 2008). However, the β-

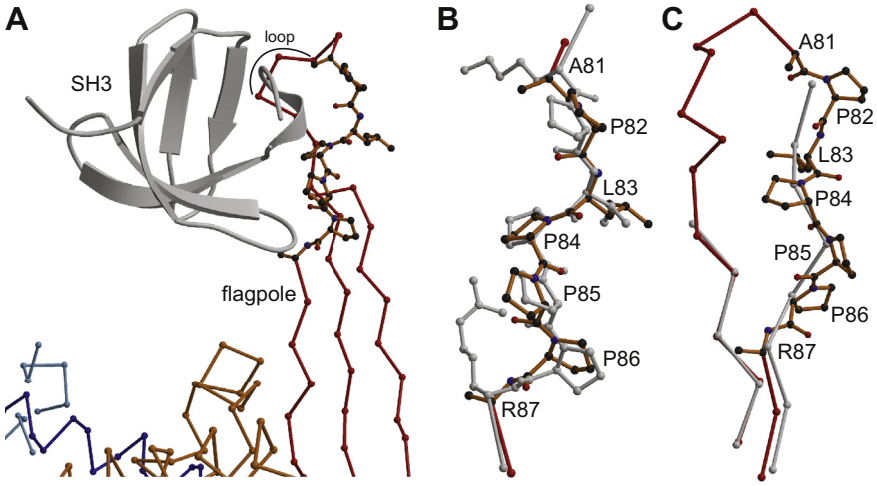

Fig.6. Model of the Rlf-SH3 domain interaction. (A) The SH3 domain of myosin I from *acanthamoeba castellanii* (pdb entry 2DRK) shown in grey was positioned onto the structure of Rlf (molecule A) based on the superposition of the bound proline-rich peptide onto residues 81–88 in Rlf, which are shown in ball-and-stick representation. The residues in the labelled loop would have to undergo slight conformation rearrangements to accommodate the docking pose of the SH3 domain. (B) Residues 80–89 of Rlf are shown with the superimposed peptide (grey). The side chain of Arg87 is not resolved in the electron density in Rlf (molecule A). (C) The loop between β1 and β2 in molecule A (red) and molecule B (grey) is shown after superposition of the flagpoles onto each other. The SH3 domain binding residues of molecule A are shown in ball-and-stick representation. (For interpretation of the references to colour in this figure legend, the reader is referred to the web version of this article.)

strands are not conserved in other cyclic nucleotide binding domains. Still, all cyclic nucleotide binding domains establish conserved interactions between the cyclic nucleotide and the domain core while unrelated C-terminal elements establish additional divergent interactions with the cyclic nucleotide (Rehmann et al., 2007; Canaves and Taylor, 2002).

Thus REM- and cyclic nucleotide binding domains are examples in which the folding units do not correspond to the functional unit. The classical definition of the REM-domain is a folding unit, but for its functionality it requires the anchor. The classical definition of the cyclic nucleotide binding domain combines the domain core, corresponding to a folding unit, with C-terminal elements that are structurally unrelated to each other (ranging form β-strands to α-helices). The flagpole-like structure in Epac2 could be considered as a folding unit serving two other folding units to acquire functionality.

The PDB database contains about 350 structures of SH3 domains, many of which in complex with a short proline-rich peptide. Only about five structures of different proteins display the interaction of a SH3 domain with more than a short proline-rich peptide and in most of these cases, the interaction is intra-molecular. It is thus of interest to analyse the interaction of SH3 domains with proline-rich motifs in the context of a full protein. On one hand the flagpole in Rlf mimics the situation of a free and short peptide, by separating the binding motif from the rest of protein. Furthermore, the flagpole fixes the six residues of the binding motif into the stretched conformation of a proline type II helix, which is required for docking of the SH3 domain, without blocking the accessibility of the residues. This is likely an important principle in gaining selectivity in signalling: identical motifs are excluded from interaction with an SH3 domain as soon as they adopt a less stretched and less accessible conformation, which might even be more common in folded proteins. Such a mechanism would put a limitation to motif predictions purely based on primary structure.

On the other hand, binding of PLCγ-1^{SH3} to the Rlf$^{75-91}$ or Rlf$^{50-514}$ is distinct thermodynamically. The lower affinity of the peptide, 16 μM instead of 0.9 μM, might be explained by additional interactions of the SH3 domain with Rlf outside the proline motif. However, the performed docking study does not support such interactions (Fig. 5). The thermodynamic characteristics are fundamentally different. Binding to the peptide is accompanied by a negative change in entropy; binding is purely driven by enthalpy. Binding to Rlf$^{50-515}$ is favoured both by enthalpy and entropy, but ΔH is only −12 kJ/mol compared to −42.5 kJ/mol observed for the peptide (Fig. 5B). This binding characteristic is in agreement with the following considerations: The isolated peptide displays a high degree of conformational freedom. The stretched conformation required for binding is only one of many possible conformations. The SH3 domain has to select the stretched conformation and to reduce conformational freedom, resulting in a decrease in entropy. If the same residues are part of the flagpole, the conformational freedom is restricted. The flagpole has fixed the residues and thereby preselected a binding conformation. The entropic price had been paid during protein folding. The pre-selection has entropic advantages but disadvantages in binding enthalpy. If bound, the isolated peptide can adopt the most optimal conformation, as for example for the formation of hydrogen bonds. The flagpole, however, constrains the residues in a preferential but not in the most optimal conformation, which reduces the binding enthalpy.

The physiological relevance of the flagpole mediated interactions remains to be determined. It is intriguing to speculate that flagpole-mediated interactions contribute to the cellular localisation of Rlf. The phospholipase PLCγ-1 is recruited to tyrosine phosphorylated transmembrane receptors via interactions of its SH2 domains (Suh et al., 2008). Rlf signalling might thus be initiated by co-translocation with PLCγ-1 independent of Ras. Alternatively, Ras•GTP might control the localisation of PLCγ-1 by using Rlf as an adaptor protein. In both cases Ral signalling would be connected to lipid signalling. Interestingly, PLCγ was recently shown to be recruited to focal adhesions based on its interaction with the guanine nucleotide exchange factors Ras-GRF1 and Ras-GRF2 (Wang et al., 2013). The interaction with intersectin-2, a guanine nucleotide exchange factor for the small G-protein CDC42 (Rossman et al., 2005), might co-ordinate Ral and CDC42 mediated effects. Finally, myosin1E associated generation of Ral•GTP might play a role in Ral controlled vesicle transport.

The crystal structure of Rlf provides insights into the determination of selectivity of SH3 domain mediated interaction. The acces-

sible exposure of the binding site and pre-selection of the binding conformation is a mechanism by which binding sites with identical primary structure, become distinguishable.

Acknowledgments

We thank Piet Gros for access to crystallisation robots, the European Synchrotron Radiation Facility for providing synchrotron facilities, the scientists at ID23eh1 for help with data collection, Cheryl Arrowsmith for providing cDNA, J.L. Bos and F.J.T. Zwartkruis for critical reading of the manuscript and our colleagues for discussion. This work was supported by Chemical Sciences of the Netherlands Organization for Scientific Research (NWO) to HR and by the TI Pharma Project T3-106 to J.L. Bos.

Appendix A. Supplementary data

Supplementary data associated with this article can be found, in the online version, at http://dx.doi.org/10.1016/j.jsb.2013.07.009.

References

Albright, C.F., Giddings, B.W., Liu, J., Vito, M., Weinberg, R.A., 1993. Characterization of a guanine nucleotide dissociation stimulator for a ras-related GTPase. EMBO J. 12, 339–347.

Boriack-Sjodin, P.A., Margarit, S.M., Bar-Sagi, D., Kuriyan, J., 1998. The structural basis of the activation of Ras by Sos. Nature 394, 337–343.

Bos, J.L., Rehmann, H., Wittinghofer, A., 2007. GEFs and GAPs: critical elements in the control of small G proteins. Cell 129, 865–877.

Canaves, J.M., Taylor, S.S., 2002. Classification and Phylogenetic Analysis of the cAMP-Dependent Protein Kinase Regulatory Subunit Family. J. Mol. Evol. 54, 17–19.

de Ruiter, N.D., Wolthuis, R.M., van, D.H., Burgering, B.M., Bos, J.L., 2000. Ras-dependent regulation of c-Jun phosphorylation is mediated by the Ral guanine nucleotide exchange factor-Ral pathway. Mol. Cell Biol. 20, 8480–8488.

Ferro, E., Magrini, D., Guazzi, P., Fischer, T.H., Pistolesi, S., Pogni, R., White, G.C., Trabalzini, L., 2008. G-protein binding features and regulation of the RalGDS family member, RGL2. Biochem. J. 415, 145–154.

Freedman, T.S., Sondermann, H., Friedland, G.D., Kortemme, T., Bar-Sagi, D., Marqusee, S., Kuriyan, J., 2006. A Ras-induced conformational switch in the Ras activator Son of sevenless. Proc. Natl. Acad. Sci. U.S.A. 103, 16692–16697.

Herrmann, C., 2003. Ras-effector interactions: after one decade. Curr. Opin. Struct. Biol. 13, 122–129.

Herrmann, C., Horn, G., Spaargaren, M., Wittinghofer, A., 1996. Differential interaction of the ras family GTP-binding proteins H-Ras, Rap1A, and R-Ras with the putative effector molecules Raf kinase and Ral-guanine nucleotide exchange factor. J. Biol. Chem. 271, 6794–6800.

Jones, T.A., Zou, J.Y., Cowan, S.W., Kjeldgaard, M., 1991. Improved methods for building protein models in electron- density maps and the location of errors in these models. Acta Crystallogr. Sect. A 47, 110–119.

Jullien-Flores, V., Mahe, Y., Mirey, G., Leprince, C., Meunier-Bisceuil, B., Sorkin, A., Camonis, J.H., 2000. RLIP76, an effector of the GTPase Ral, interacts with the AP2 complex: involvement of the Ral pathway in receptor endocytosis. J. Cell Sci. 113 (Pt 16), 2837–2844.

Kabsch, W., 1993. Automatic processing of rotation diffraction data from crystals of initially unknown symmetry and cell constants. J. Appl. Crystallogr. 26, 795–800.

Kay, B.K., Williamson, M.P., Sudol, M., 2000. The importance of being proline: the interaction of proline-rich motifs in signaling proteins with their cognate domains. FASEB J. 14, 231–241.

Kraulis, P.J., 1991. Molscript - a program to produce both detailed and schematic plots of protein structures. J. Appl. Crystallogr. 24, 946–950.

Merritt, E.A., Murphy, M.E.P., 1994. Raster3D version-2.0 - A program for photorealistic molecular graphics. Acta Crystallogr. Sect. D: Biol. Crystallogr. 50, 869–873.

Moskalenko, S., Henry, D.O., Rosse, C., Mirey, G., Camonis, J.H., White, M.A., 2002. The exocyst is a Ral effector complex. Nat. Cell Biol. 4, 66–72.

Murai, H., Ikeda, M., Kishida, S., Ishida, O., Okazaki-Kishida, M., Matsuura, Y., Kikuchi, A., 1997. Characterization of Ral GDP dissociation stimulator-like (RGL) activities to regulate c-fos promoter and the GDP/GTP exchange of Ral. J. Biol. Chem. 272, 10483–10490.

Murshudov, G.N., Vagin, A.A., Dodson, E.J., 1997. Refinement of macromolecular structures by the maximum-likelihood method. Acta Crystallogr. D. Biol. Crystallogr. 53, 240–255.

Quilliam, L.A., Rebhun, J.F., Castro, A.F., 2002. A growing family of guanine nucleotide exchange factors is responsible for activation of Ras-family GTPases. Prog. Nucleic Acid Res. Mol. Biol. 71, 391–444.

Rehmann, H., 2006. Characterization of the activation of the Rap-specific exchange factor Epac by cyclic nucleotides. Methods Enzymol. 407, 159–173.

Rehmann, H., Arias-Palomo, E., Hadders, M.A., Schwede, F., Llorca, O., Bos, J.L., 2008. Structure of Epac2 in complex with a cyclic AMP analogue and RAP1B. Nature 455, 124–127.

Rehmann, H., Das, J., Knipscheer, P., Wittinghofer, A., Bos, J.L., 2006. Structure of the cyclic-AMP-responsive exchange factor Epac2 in its auto-inhibited state. Nature 439, 625–628.

Rehmann, H., Wittinghofer, A., Bos, J.L., 2007. Capturing cyclic nucleotides in action: snapshots from crystallographic studies. Nat. Rev. Mol. Cell Biol. 8, 63–73.

Rossman, K.L., Der, C.J., Sondek, J., 2005. GEF means go: turning on RHO GTPases with guanine nucleotide-exchange factors. Nat. Rev. Mol. Cell Biol. 6, 167–180.

Schomburg, D., Reichelt, J., 1988. Bragi - A Comprehensive Protein Modeling Program System. J. Mol. Graphics 6, 161–165.

Sondermann, H., Soisson, S.M., Boykevisch, S., Yang, S.S., Bar-Sagi, D., Kuriyan, J., 2004. Structural analysis of autoinhibition in the Ras activator Son of sevenless. Cell 119, 393–405.

Suh, P.G., Park, J.I., Manzoli, L., Cocco, L., Peak, J.C., Katan, M., Fukami, K., Kataoka, T., Yun, S., Ryu, S.H., 2008. Multiple roles of phosphoinositide-specific phospholipase C isozymes. BMB. Rep. 41, 415–434.

Urano, T., Emkey, R., Feig, L.A., 1996. Ral-GTPases mediate a distinct downstream signaling pathway from Ras that facilitates cellular transformation. EMBO J. 15, 810–816.

Vagin, A., Teplyakov, A., 2000. An approach to multi-copy search in molecular replacement. Acta Crystallogr. D: Biol. Crystallogr. 56 (Pt 12), 1622–1624.

Vetter, I.R., Wittinghofer, A., 2001. The guanine nucleotide-binding switch in three dimensions. Science 294, 1299–1304.

Wang, Q., Siminovitch, K.A., Downey, G.P., McCulloch, C.A., 2013. Ras-guanine-nucleotide-releasing factors 1 and 2 interact with PLCgamma at focal adhesions to enable IL-1-induced Ca2+ signalling, ERK activation and MMP-3 expression. Biochem. J. 449, 771–782.

Wennerberg, K., Rossman, K.L., Der, C.J., 2005. The Ras superfamily at a glance. J. Cell Sci. 118, 843–846.

White, M.A., Vale, T., Camonis, J.H., Schaefer, E., Wigler, M.H., 1996. A role for the Ral guanine nucleotide dissociation stimulator in mediating Ras-induced transformation. J. Biol. Chem. 271, 16439–16442.

Wolthuis, R.M., de Ruiter, N.D., Cool, R.H., Bos, J.L., 1997. Stimulation of gene induction and cell growth by the Ras effector Rlf. EMBO J. 16, 6748–6761.